Metamaterials with engineered failure load and stiffness

Sai Sharan Injeti[a], Chiara Daraio[a], and Kaushik Bhattacharya[a,1]

[a]Department of Mechanical and Civil Engineering, California Institute of Technology, Pasadena, CA 91125

Edited by David A. Weitz, Harvard University, Cambridge, MA, and approved October 21, 2019 (received for review July 9, 2019)

Architected materials or metamaterials have proved to be a very effective way of making materials with unusual mechanical properties. For example, by designing the mesoscale geometry of architected materials, it is possible to obtain extremely high stiffness-to-weight ratio or unusual Poisson's ratio. However, much of this work has focused on designing properties like stiffness and density, and much remains unknown about the critical load to failure. This is the focus of the current work. We show that the addition of local internal prestress in selected regions of architected materials enables the design of materials where the critical load to failure can be optimized independently from the density and/or quasistatic stiffness. We propose a method to optimize the specific load to failure and specific stiffness using sensitivity analysis and derive the maximum bounds on the attainable properties. We demonstrate the method in a 2D triangular lattice and a 3D octahedral truss, showing excellent agreement between experimental and theoretical results. The method can be used to design materials with predetermined fracture load, failure location, and fracture paths.

metamaterials | lattices | architected structures | failure | optimal properties

It has long been understood that material microstructure or microgeometry affects its overall or engineering property, and this has been exploited in composite materials, sandwich structures, and cellular materials (1–3). There are well-established engineering approaches (4) and rigorous mathematical results (2, 5) that have studied the problem of finding bounds on mechanical properties and identifying optimal microstructures that attain them. However, until recently, the ability to fabricate materials with controlled microgeometry was limited. The advent of 3D printing and similar approaches of materials synthesis with highly controlled geometries have overcome this limitation (6) and opened the doors for engineering architected materials or metamaterials with unusual mechanical properties (7, 8).

A topic that has received particular attention is designing and synthesizing materials that maximize stiffness for a given density (9–20). A recent result demonstrated that it is possible to approach the Hashin–Shtrikhman bounds with a single-scale architected material (7), although hierarchical structures were known earlier (21). Another topic that has received much attention is the development of architected materials with unusual (negative) Poisson's ratio (22–24). Note that both of these properties concern aspects of the overall linear elastic modulus. Indeed, Milton and Cherkaev (25) have studied all possible elastic moduli that can be attained by lattices, and identified a pentamode material.

Still, much remains unknown about failure for many reasons. Failure depends on the local state of stress and is therefore difficult to characterize from a theoretical point of view. Further, failure is sensitive to defects and imperfections. Finally, there are no general bounds on failure. However, failure is critically important from the point of view of application. Typically, the critical load to failure increases with stiffness, and this leaves a gaping hole in the space of possible material properties as shown in Fig. 1*A*. Fig. 1 shows the specific stiffness and specific failure load of various materials systems; note that there are no materials that have high specific load to failure but limited stiffness indicated by the dashed ellipse.

In this work, we show using trusses that this gap can be bridged. In particular, we show that the critical load to failure in a truss can be varied within a range while holding the stiffness and density fixed. We do so by exploiting states of self-stress in a truss. A truss is a structure made of elongated members or bars joined together at nodes that can transmit force but not moments. Depending on the topology of a truss, it may have mechanisms whereby some nodes are free to move or it can support states of self-stress. Fig. 1*B* shows an octet truss with self-stress—the bars in blue are in compression while the bars in red are in tension. We show that states of self-stress can be exploited to increase the critical load to failure. We then derive bounds on the range of specific (per unit relative density) stiffness and specific load to failure. Here, the relative density of a truss is defined by the ratio of density of the lattice to the density of the material from which it is constructed. We validate the results from numerical simulations using experiments in both two- and three-dimensions.

Our work is related to other ideas in the literature. Paulouse et al. (26) showed using the 3D version of a Kagome lattice that they can control the nonlinear mechanical response by selectively activating buckling modes using states of self-stress. Our focus here is on tensile fracture rather than compressive buckling. Mishuris and Slepyan (27) showed that the peak stress in a self-equilibrated 1D chain of stretched and compressed bonds can be controlled by varying the internal stresses. Our idea is similar, but addresses higher dimensions. Rao et al. (28) proposed the idea of using residual stresses, to delay failure in composites and ceramics. We apply a similar concept to architected materials.

Optimization of Specific Failure Load and Specific Stiffness

A pin-jointed truss is a structure made of linear bars that carry uniaxial (tensile or compressive) force held together by joints that transmit force but no moment. The truss is called statically

Significance

A structure that fails at large loads is expected to be dense and stiff. This is because in conventional materials failure load depends directly on stiffness and density. This paper shows that the addition of engineered internal stresses in truss-like structures allows decoupling of these properties, increasing the failure load 2-fold while maintaining constant the density and stiffness. A similar approach could also be used to control locations and paths of failure in architected materials.

Author contributions: S.S.I., C.D., and K.B. designed research; S.S.I. performed research; S.S.I., C.D., and K.B. contributed new reagents/analytic tools; S.S.I., C.D., and K.B. analyzed data; and S.S.I., C.D., and K.B. wrote the paper.

The authors declare no competing interest.

This article is a PNAS Direct Submission.

[1]To whom correspondence may be addressed. Email: bhatta@caltech.edu.

This article contains supporting information online at www.pnas.org/lookup/suppl/doi:10.1073/pnas.1911535116/-/DCSupplemental.

First published November 11, 2019.

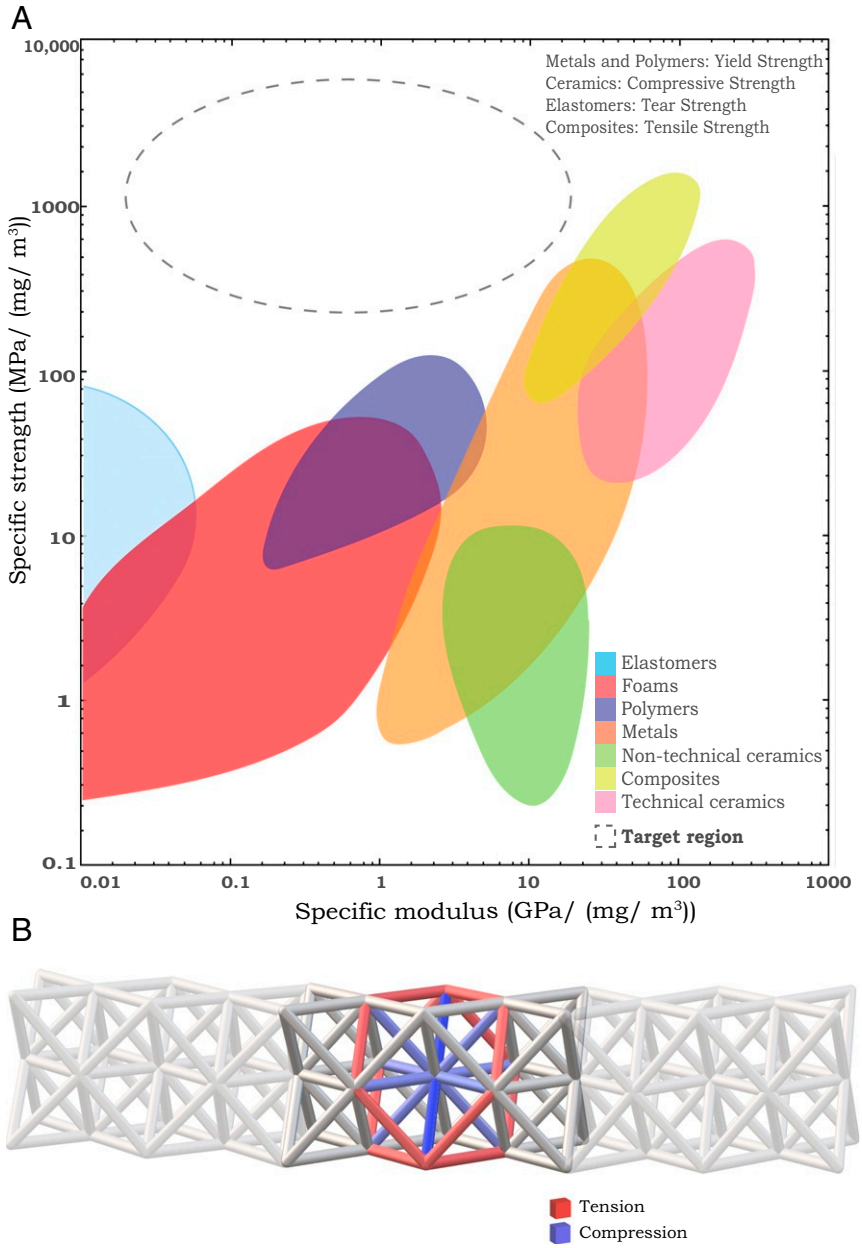

Fig. 1. (*A*) Material selection chart of specific modulus (ratio of Young's modulus of elasticity E to density ρ) versus specific strength (ratio of stress at failure σ_f to ρ) for different materials/structures according to data obtained from ref. 29. (*B*) Example of an internally stressed octet truss with 2 unit cells (darker gray members and colored bars). Red and blue elements illustrate the distribution of a state of self-stress.

determinate if the force in each bar can be calculated only from static equilibrium equations given the external loads. If there are too many bars such that the equilibrium conditions are insufficient to determine the forces in the members, the truss is statically indeterminate. Such a structure can be internally stressed, even when there are no external loads. An analysis going back to Maxwell (30) and subsequently generalized (31) shows that

$$b - nd + 3(d-1) = s - m, \qquad [1]$$

where b is the number of bars, n the number of joints, d the dimension (2 or 3), s the number of linearly independent (modes) of self-stress, and m the number of independent mechanisms. In a self-stressed system, some members are in tension while others are in compression, but the whole structure is in equilibrium without any external loads. In our analysis, we consider a statically indeterminate truss with s states of self-stress. We define s_α^j the stress in the αth bar due to the jth state of self-stress, $\alpha = 1, \ldots, b$, $j = 1, \ldots, s$. So the stress in the αth bar is $\sum_j \lambda_j s_\alpha^j$, where λ_j is the intensity of the jth state of self-stress.

In designing architected materials, the octet truss has played a predominant role among space-filling structures, since it exhibits high stiffness and strength that scale linearly with its relative density (at low relative densities). Also, the structure has a nodal connectivity of 12, making it highly indeterminate with a stretch-dominated mechanical response (32). These properties make it a prime example for our analysis. We study the octahedral truss with 6 unit cells and 9 states of self-stress (Fig. 2*A*) and the octet truss with 2 unit cells and 5 states of self-stress (Figs. 1*B* and 2

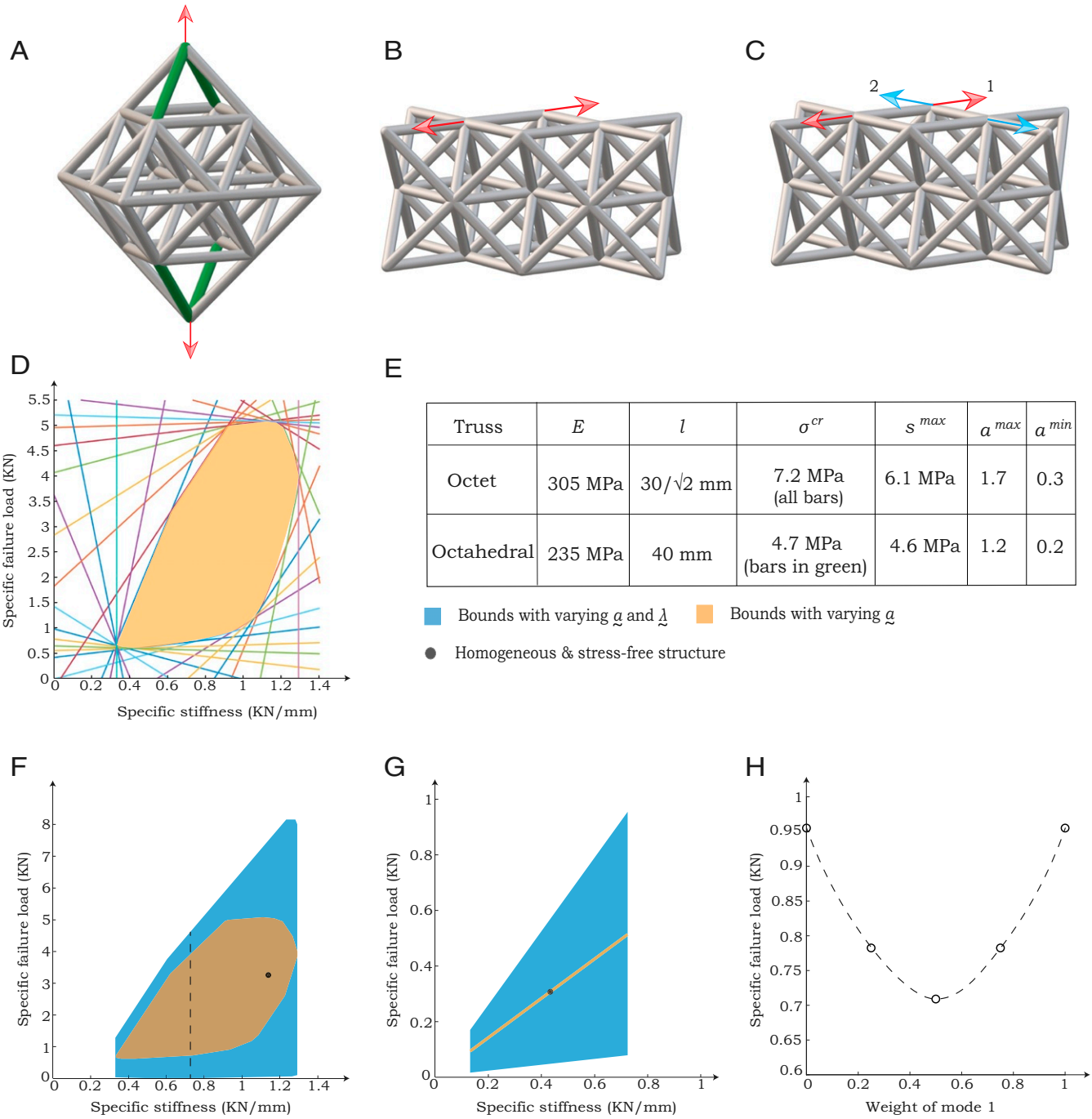

Fig. 2. (*A*) Octahedral truss loaded along a single mode, in which failure occurs in a bar in green. (*B* and *C*) Octet truss loaded along a single mode and 2 modes, respectively, where any bar can fail in tension. (*D*) Construction of bounds on specific (per unit relative density) failure load and specific stiffness for the octahedral truss with varying cross-sectional areas alone. (*E*) Table indicating parameters of optimization for both trusses. $s^{\max}$ represents the maximum allowed magnitude of prestress in a bar. $a^{\max}$ and $a^{\min}$ are the maximum and minimum values a_α can take. (*F* and *G*) Calculated bounds on attainable specific load to failure and specific stiffness, for the octahedral truss and octet truss loaded along a single mode. The dashed line indicates the specific stiffness of the octahedral truss experimentally tested. (*H*) Variation of maximum value of weighted specific failure load with weight associated to mode 1, for the octet truss with 2 symmetric loading modes.

B and *C*). The octahedral truss considered is still a portion of a larger octet truss, with several unit cells stacked together in all 3 dimensions.

Now suppose the truss is subjected to a particular mode of loading (e.g., Fig. 2*A*) with an applied force T. We solve the equations of equilibrium as described in *SI Appendix*, and obtain the force carried by the αth bar to be Tf_α, where f_α is a dimensionless quantity depending on the topology of the truss. The total force in this bar is $Tf_\alpha + \sum_j \lambda_j A_\alpha s_\alpha^j$, where A_α is the cross-sectional area of the αth bar. The whole structure is safe if this force does not exceed the positive critical failure load in tension (e.g., yielding or fracture) $F_\alpha^{\mathrm{cr}(1)} = A_\alpha \sigma_\alpha^{\mathrm{cr}(1)}$ and does not drop below the negative critical failure load in compression (e.g., buckling) $F_\alpha^{\mathrm{cr}(2)} = A_\alpha \sigma_\alpha^{\mathrm{cr}(2)}$, in that bar. It follows that the failure load—the applied load at which any bar fails—is given by

$$T_{\text{cr}} = \min_{i\in\phi}\left\{ A \min_{\beta\in\beta^{(i)}} a_\beta \frac{\sigma_\beta^{\text{cr(i)}} - \sum_j \lambda_j s_\beta^j}{f_\beta} \right\}, \quad \textbf{[2]}$$

where $\phi = \{1, 2\}$, $\beta^{(1)} = \{\beta:\ f_\beta > 0\}$, and $\beta^{(2)} = \{\beta:\ f_\beta < 0\}$. We denote $A_\alpha = Aa_\alpha$ for some nondimensional area ratio a_α. Further, the stiffness/modulus of the structure is given by

$$M = \frac{A}{\sum_\alpha \frac{l_\alpha f_\alpha^2}{E a_\alpha}}, \quad \textbf{[3]}$$

where l_α is the length of the αth bar and E the elastic modulus of the solid material.

It is possible to show that the relative density, $\overline{\rho}$ of a truss with fixed length of the bars scales as A, as long as $\sum_\alpha a_\alpha = b$ so that $\overline{\rho} = A\rho_o$, where ρ_o depends on the truss geometry and length of a bar. In particular, if all of the bars are uniform (with length l and cross-sectional area A), the relative density is $6\frac{\sqrt{2}A}{l^2}$ $(7\frac{A}{\sqrt{2}l^2})$ for the octet (octahedral) truss in Fig. 2.

Therefore, we obtain the expressions for the specific failure load (ratio of failure load to relative density) and specific stiffness (ratio of stiffness to relative density) as

$$\overline{T}_{\text{cr}} = \min_{i\in\phi}\left\{ \min_{\beta\in\beta^{(i)}} \frac{a_\beta}{\rho_o} \frac{\sigma_\beta^{\text{cr(i)}} - \sum_j \lambda_j s_\beta^j}{f_\beta} \right\}, \quad \textbf{[4]}$$

$$\overline{M} = \frac{1}{\rho_o} \frac{1}{\sum_\alpha \frac{l f_\alpha^2}{E a_\alpha}}. \quad \textbf{[5]}$$

Previous work has considered optimizing and bounding the specific stiffness $\overline{M}$ by varying the nondimensional cross-sectional areas a_α subject to the constraint $\sum_\alpha a_\alpha = b$. In this work, we focus on a combination of the specific stiffness $\overline{M}$ and specific failure load $\overline{T}_{\text{cr}}$, while varying nondimensional area a_α $(\sum a_\alpha = b)$ and prestress λ_j. A difficulty in doing so is that the specific failure load is itself defined through a variational principle—this makes the usual approaches to optimization which requires the computation of the sensitivity difficult. Therefore, we approximate it as

$$\overline{T}_{\text{cr}} \approx \left(\sum_{i\in\phi} \left(\sum_{\beta\in\beta^{(i)}} \left(\frac{a_\beta}{\rho_o} \frac{\sigma_\beta^{\text{cr(i)}} - \sum_j \lambda_j s_\beta^j}{f_\beta} \right)^{-p} \right) \right)^{-1/p}, \quad \textbf{[6]}$$

for p large enough (we take $p = 5$ in our calculations).

In the rest of this section, we find bounds on all possible values of $\overline{T}_{\text{cr}}, \overline{M}$ that can be obtained by changing a_α, λ_j considering failure of a bar in tension alone, i.e., $\phi = 1$. However, it is straightforward to extend the analysis to include bars failing due to compressive stresses using Eq. **6** with $\phi = \{1, 2\}$. Given any γ_1 and γ_2, we maximize the objective function $\mathcal{O} = \gamma_1 \overline{T}_{\text{cr}} + \gamma_2 \overline{M}$ to find $\mathcal{O}^{\max}$ using established methods (we find the sensitivity using the adjoint method and avoid local minima by taking multiple initial guesses; details in *SI Appendix*). It then follows that for any given $\{a_\alpha, \lambda_j\}$, $\gamma_1 \overline{T}_{\text{cr}}(a_\alpha, \lambda_j) + \gamma_2 \overline{M}(a_\alpha, \lambda_j)$ lies in the half plane $\gamma_1 \overline{T}_{\text{cr}} + \gamma_2 \overline{M} \le \mathcal{O}^{\max}$. The intersection of all such half planes (for all values of γ_1, γ_2) defines an outer bound on all possible values of $\overline{T}_{\text{cr}}(a_\alpha, \lambda_j), \overline{M}(a_\alpha, \lambda_j)$. This construction is shown in Fig. 2*D*, using the constraints on design mentioned in Fig. 2*E*. It is an outer bound because all attainable values lie in the set, but it is not guaranteed by the argument above that all points inside the set are feasible. However, the points on the boundary that correspond to unique points where the tangent touches the set are in fact feasible; i.e., it is possible to find the distribution of nondimensional areas a_α and intensities of states of self-stress λ_j that result in specific failure load and specific stiffness indicated by these points. This is important because extremal properties are likely to occur at such points.

Our analysis shows that it is possible to significantly expand the attainable specific failure load and specific stiffness values in trusses, by varying the nondimensional areas and prestress of the bars (Fig. 2 *F* and *G*). The points marked in black in Fig. 2 *F* and *G* indicate the specific failure load and specific stiffness for a uniform truss with no prestress. The yellow region (line in the case of the octet truss) gives bounds on all possible values of specific failure load and specific stiffness that can be obtained by varying the nondimensional areas while keeping the prestress uniformly zero (i.e., varying a_α subject to the constraint $\sum_\alpha a_\alpha = b$ with $\lambda_j = 0$). The blue region gives bounds on all possible values of specific failure load and specific stiffness that can be obtained by varying both nondimensional areas and prestress (i.e., varying a_α subject to the constraint $\sum_\alpha a_\alpha = b$ and λ_j). Here, the prestress does not affect the range of specific stiffness that the truss can attain. Instead, internal stresses can significantly increase the specific failure load. By varying the distributions of nondimensional areas and prestress, one can increase the specific stiffness of the octet truss by a factor of 2 and simultaneously increase its specific failure load by a factor of 3, within the constraints of design mentioned in Fig. 2*E*.

Finally, we study the case in which an octet truss is loaded in multiple modes (Fig. 2*C*). In such situations, it is natural to seek the Pareto optimal, or the envelope of optimal values, for various weights of the different loading modes. Consider r loading modes and suppose we assign weights/intensities $w_i,\ i = 1, \ldots r, w_i > 0,\ \sum w_i = 1$ for the different modes. Then, the formulas above for failure of a bar in tension are easily generalized as

$$\overline{T}_{\text{cr}} = \sum_i w_i \min_{\{\beta:\ f_{i,\beta} > 0\}} \frac{a_\beta}{\rho_o} \frac{\sigma_\beta^{\text{cr}} - \sum_j \lambda_j s_\beta^j}{f_{i,\beta}}, \quad \textbf{[7]}$$

$$\overline{M} = \sum_i \frac{w_i}{\rho_o} \frac{1}{\sum_\alpha \frac{l f_{i,\alpha}^2}{E a_\alpha}}, \quad \textbf{[8]}$$

where $\sigma_\beta^{\text{cr}} = \sigma_\beta^{\text{cr(1)}}$. We find the Pareto optimal by considering all possible weights. Fig. 2*H* shows representative results for the octet truss for a combination of 2 modes of loading shown in Fig. 2*C*.

In this section, we calculated bounds on attainable specific failure load and specific stiffness. However, to design a truss with a particular property within these bounds, one can minimize a norm of the difference between Eq. **4** or Eq. **5** and the required property using a sensitivity analysis similar to the one described in *SI Appendix*. We would then arrive at distributions a_α and λ_j that result in specific failure load/stiffness close to or at the desired value. For a truss with a given relative density $\overline{\rho}$ and nondimensional area distribution a_α, the distribution of cross-sectional areas of bars can be calculated as $A_\alpha = Aa_\alpha$, where $\overline{\rho} = A\rho_o$.

We note that this previous analysis concerns ideal truss-like structures and thus applies to lattices at low relative densities (33–35). Since lattice structures are to be used for lightweight structures, the low relative densities are of substantial interest. Further, while additional issues arise at higher relative densities, the basic principle of using prestress to optimize failure load remains valid even though the formulation requires refinement as the members can support moments.

Experimental Results

To demonstrate the principles described above, we first choose a triangular lattice (Fig. 3*A*), which is part of a planar section of the octet truss with several unit cells stacked along 2 directions.

This geometry is statically indeterminate with 3 states of self-stress. We then validate the model in 3 dimensions, using an octahedral truss, with 9 states of self-stress (Fig. 3*B*). Since prior work has studied stiffness in detail (20), here we focus on maximizing the failure load with respect to the distribution of internal stress λ_j for a given distribution of area a_α and relative density $\overline{\rho}$. Internal stress distributions as a result of this optimization (see algorithm in *SI Appendix*) are qualitatively indicated on samples in Fig. 3 *A* and *B*. The bars in red are in tension while those in blue are under compression. The octahedral truss considered here has a specific stiffness value and maximized specific failure load that lie on the dashed line indicated in Fig. 2*F*. The specimens are fabricated using a Stratasys Connex500 multimaterial 3D printer, with the bars made of DM8530-GREY60 material with tapered cross-sections at the joints that are then reinforced with a much softer TangoBlackPlus (TB) (36). This ensures that the assumption of ideal pin-jointed structures remains valid, even though the relative density of the octahedral truss is 5.7%, which may be close to the limit of validity for unmodified lattices (33–35). The length of each bar is 40 mm.

Any statically indeterminate structure can be internally prestressed to a desired distribution, by inducing local prestrain in selected bars. This is possible because the principle of superposition applies in the limit of small deformations. In our examples, we introduce local precompression in 3 of the bars in the triangular lattice and in 4 bars of the octahedral truss. These bars (indicated by green arrowheads in Fig. 3 *A* and *B*) are initially precompressed, but are then subjected to tensile stresses when the truss is loaded. The magnitude of the local precompression on these bars is determined using superposition, so that the final stress state of the lattices matches the desired distribution of self-stress, obtained from numerical simulations (*SI Appendix*).

To emulate the effect of local precompression, we introduce hinge mechanisms in the center of these bars, allowing them to buckle slightly and remain unstressed before loading is applied. We call such bars the slack bars (Fig. 3*C*). The amount of slack in each mechanism is designed to match the displacement needed for its locally precompressed bar to reach zero stress. Hence, as the structure is loaded, the tensile displacements in the mechanism compensate the slack, eventually engaging the pins in each hinge. From this point onward, the stress state of the truss is identical to that expected from the desired prestressed structure under the same load. We verify this experimentally by ensuring that the global effective stiffness of the structures tested matches the expected values. In control experiments, we introduce hinges

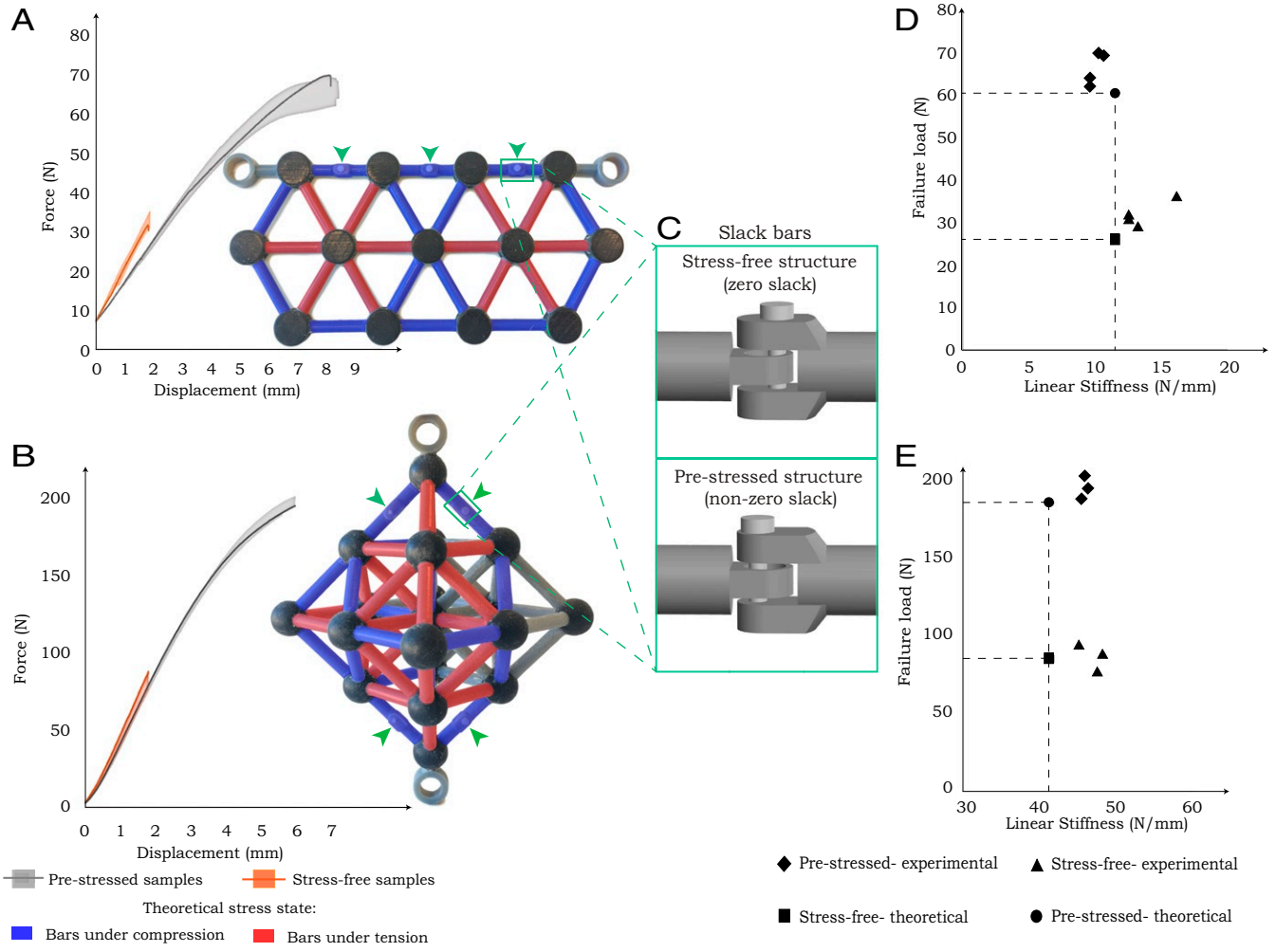

Fig. 3. (*A* and *B*) Experimental results from tensile tests on the triangular lattice and octahedral truss, respectively. The solid line indicates the data for a particular specimen, while the shaded area indicates all test data. (*C*) Close-up of the hinge that enables the slack bar—note that the position of the pin is changed. (*D* and *E*) The failure load and stiffness—both experimental and theoretical—for the specimens with and without prestress for the triangular lattice and octahedral truss, respectively.

with no slack, to test failure of structures with no initial prestress. Importantly, the hinge mechanisms also act as defects in the bars and localize failure due to tensile stresses away from the joints of the truss, at a fixed load level.

The lattices are tested in an Instron testing machine, operated in displacement control. The results of the tensile tests, performed to failure for both the triangular lattice (Fig. 3*A*) and the octahedral truss (Fig. 3*B*), show a significant difference between the samples with and without slack in the hinge mechanisms. The resulting stiffness and failure load are compared to the theoretically predicted values (Fig. 3 *D* and *E*), showing excellent agreement. To obtain the theoretical values, individual bars are fabricated using the same method and tested in tension at the same strain rate. We obtain a linear stiffness of 115.28 ± 1.91 N/mm and 21.12 ± 0.64 N/mm for the regular and the slack bar, respectively, and the maximum load to failure in the slack bar is 15.12 ± 1.56 N.

We obtain a 2-fold increase (107.21% for the triangular lattice and 127.44% for the octahedral truss) in the specific failure load of the prestressed structures, compared to the structures with no prestress. However, the stiffness of the structures with and without prestress remains almost constant, as intended. Consequently there is a 4-fold increase in the work of fracture.

Discussion

Our analysis expresses failure load of architected materials in terms of geometrical parameters that can be used in design. This approach decouples stiffness from strength and allows the calculation of global optima using sensitivity analysis. As stiffness and failure load scale linearly with density, for stretch-dominated structures at low relative densities, the approach can be used to design arbitrarily lightweight structures. We show that the design bounds can be reached in truss-like structures, introducing internal stresses and varying the distribution of cross-sectional areas within the structures. We demonstrate this technique on the octet and octahedral trusses. While these are relatively simple examples, they illustrate the principle. The formulas and the methods presented are applicable to trusses of arbitrary complexity.

The analysis and approach can be generalized in multiple ways. First, for lattices with higher relative density, the analysis has to take into account the bending and the shear forces. While the principle of using prestress remains valid, Eqs. **2**–**8** need to be refined. Second, our analysis uses first failure as our failure criterion. This is of interest in application due to reliability concerns. However, there are situations where one may use the failure of the entire structure as the failure criterion. This may lead to degeneracies and one may have to optimize over all possible failure sequences. Third, the proposed design approach could be further extended, to include more complicated loading conditions (e.g., complex loading histories or dynamic solicitations) and expand materials' functionalities. For example, engineering prestress can be used to improve impact energy absorption and failure of architected foams. The addition of prestresses can also be an important tool to engineer large shape changes in materials (37). Finally, internally stressed structures can be studied to create predetermined failure paths in a structure, which can be useful to prolong the life of a product.

Data Availability. All data needed to evaluate the conclusions in this paper are available in the main text or in *SI Appendix*.

ACKNOWLEDGMENTS. We thank Petros Arakelian for helping print the samples used for this research. We also thank Connor McMahan and Dr. Osama Bilal for useful discussions on the experiments. This work was supported by the Shang-Li and Betty Huang endowed graduate fellowship fund in mechanical engineering at the California Institute of Technology. C.D. acknowledges support from the National Science Foundation (NSF) CSSI Grant 1835735.

1. J. R. Vinson, *The Behavior of Sandwich Structures of Isotropic and Composite Materials* (CRC Press, 1999).
2. G. W. Milton, *The Theory of Composites* (Cambridge University Press, 2002).
3. L. J. Gibson, M. F. Ashby, *Cellular Solids, Structure and Properties* (Cambridge University Press, 1997).
4. S. Nemat-Nasser, M. Hori, *Micromechanics: Overall Properties of Heterogeneous Materials* (North-Holland, 1999).
5. G. W. Milton. Stiff competition. *Nature* **564**, E1 (2018).
6. I. Gibson, D. W. Rosen, S. Brent, *Additive Manufacturing Technologies* (Springer, Berlin, Germany, 2010).
7. J. B. Berger, H. N. G. Wadley, R. M. McMeeking, Mechanical metamaterials at the theoretical limit of isotropic elastic stiffness. *Nature* **543**, 533–537 (2017).
8. M. Kadic, G. W. Milton, M. Hecke, M. Wegener, 3D metamaterials. *Nat. Rev. Phys.* **1**, 198–210 (2019).
9. L. J. Gibson, M. F. Ashby, *Cellular Solids: Structure and Properties* (Cambridge University Press, 1990).
10. H. Fan *et al.*, Modulus-density scaling behaviour and framework architecture of nanoporous self-assembled silicas. *Nat. Mater.* **6**, 418–423 (2007).
11. J. A. Kepler, Simple stiffness tailoring of balsa sandwich core material. *Compos. Sci. Technol.* **71**, 46–51 (2011).
12. T. A. Schaedler *et al.*, Ultralight metallic microlattices. *Science* **334**, 962–965 (2011).
13. K. Tantikom, T. Aizawa, Compressive deformation simulation of regularly cell-structured materials with various column connectivity. *Mater. Trans.* **46**, 1154–1160 (2005).
14. A. Torrents, T. A. Schaedler, A. J. Jacobsen, W. B. Carter, L. Valdevit, Characterization of nickel-based microlattice materials with structural hierarchy from the nanometer to the millimeter scale. *Acta Mater.* **60**, 3511–3523 (2012).
15. C. Q. Dam, R. Brezny, D. J. Green, Compressive behavior and deformation-mode map of an open cell alumina. *J. Mater. Res.* **5**, 163–171 (1990).
16. J. K. Cochran, K. J. Lee, D. McDowell, T. Sanders, "Multifunctional metallic honeycombs by thermal chemical processing" in *Processing and Properties of Lightweight Cellular Metals and Structures, Global Symposium on Materials Processing and Manufacturing, 3, TMS Annual Meeting*, A. K. Ghosh, T. H. Sanders, T. D. Claar, Eds. (The Minerals, Metals & Materials Society (TMS), Seattle, WA, 2002), pp. 127–136.
17. J. Zhang, M. F. Ashby, The out-of-plane properties of honeycombs. *Int. J. Mech. Sci.* **34**, 475–489 (1992).
18. D. Rayneau-Kirkhope, Y. Mao, R. Farr, Ultralight fractal structures from hollow tubes. *Phys. Rev. Lett.* **109**, 204301 (2012).
19. K. C. Cheung, N. Gershenfeld, Reversibly assembled cellular composite materials. *Science* **341**, 1219–1221 (2013).
20. M. Philip Bendsoe, O. Sigmund, *Topology Optimization: Theory, Methods and Applications* (Springer, 2004).
21. G. A. Francfort, F. Murat, Homogenization and optimal bounds in linear elasticity. *Arch. Ration. Mech. Anal.* **94**, 307–334 (1986).
22. D. R. Reid *et al.*, Auxetic metamaterials from disordered networks. *Proc. Natl. Acad. Sci. U.S.A.* **115**, E1384–E1390 (2018).
23. K. E. Evans, A. Alderson, Auxetic materials: Functional materials and structures from lateral thinking!*Adv. Mater.* **12**, 617–628 (2000).
24. T. Bückmann *et al.*, Tailored 3D mechanical metamaterials made by dip-in direct-laser-writing optical lithography. *Adv. Mater.* **24**, 2710–2714 (2012).
25. G. W. Milton, A. V. Cherkaev, Which elasticity tensors are realizable? *J. Eng. Mater. Technol.* **117**, 483–493 (1995).
26. J. Paulose, S. A. Meeussen, V. Vitelli, Selective buckling via states of self-stress in topological metamaterials. *Proc. Natl. Acad. Sci. U.S.A.* **112**, 7639–7644 (2015).
27. G. S. Mishuris, L. I. Slepyan, Brittle fracture in a periodic structure with internal potential energy. *Proc. Math. Phys. Eng. Sci.* **470**, 20130821 (2014).
28. M. P. Rao, A. J. Sanchez-Herencia, G. E. Beltz, R. M. McMeeking, F. F. Lange, Laminar ceramics that exhibit a threshold strength. *Science* **286**, 102–105 (1999).
29. M. Wenzelburger, M. Silber, D. Gadow, Manufacturing of light metal matrix composites by combined thermal spray and semisolid forming process – Summary of the current state of technology. *Key Eng. Mater.* **425**, 217–244 (2010).
30. J. C. Maxwell. On the calculation of the equilibrium and stiffness of frames. *Lond. Edinb. Dublin Philos. Mag. J. Sci.* **27**, 294–299 (1864).
31. M. F. Ashby *et al.*, Metal foams: A design guide. *Mater. Des.* (Butterworth-Heinemann, 2002).
32. V. S. Deshpande, N. A. Fleck, M. F. Ashby. Effective properties of the octet-truss lattice material. *J. Mech. Phys. Solids* **49**, 1747–1769 (2001).
33. S. Watts, W. Arrighi, J. Kudo, D. A. Tortorelli, D. A. White, Simple, accurate surrogate models of the elastic response of three-dimensional open truss micro-architectures with applications to multiscale topology design. *Struct. Multidiscip. Optim.*, 10.1007/s00158-019-02297-5 (2019).
34. L. R. Meza *et al.*, Reexamining the mechanical property space of three-dimensional lattice architectures. *Acta Mater.* **140**, 424–432 (2017).
35. L. Dong, V. Deshpande, H. Wadley. Mechanical response of Ti-6Al-4V octet-truss lattice structures. *Int. J. Solids Struct.* **60–61**, 107–124 (2015).
36. J. E. M. Teoh *et al.*, Design and 4d printing of cross-folded origami structures: A preliminary investigation. *Materials* **11**, E376 (2018).
37. A. A. Bauhofer *et al.*, Harnessing photochemical shrinkage in direct laser writing for shape morphing of polymer sheets. *Adv. Mater.* **29**, 1703024 (2017).